ADV MATH SCI JOURNAL

Advances in Mathematics: Scientific Journal **10** (2021), no.2, 743–758
ISSN: 1857-8365 (printed); 1857-8438 (electronic)
https://doi.org/10.37418/amsj.10.2.6

A NEW PRE-PROCESSING TECHNIQUE FOR COMPUTATIONAL OF STEREO MATCHING ALGORITHM

A. F. Kadmin, R. A. Hamzah[1], N. A. Manap, and M. S. Hamid

ABSTRACT. This paper presents a new composition of stereo vision algorithm for disparity map measurement from matching process. Stereo colour images obtained are consists with noises due to undesirable weather and illumination conditions due to it taken under inadequate or non-uniform light. The algorithm begins with pre-processing stage to enhance the colour image quality using combination of CLAHE, AGCWD and guided filter. Then, the matching cost computation are done using the Census Transform that has a strong advantage in radial distortion and brightness changes. The third stage will produce the aggregated cost from matching process utilizing fixed-window and guided filter technique. At the fourth stage; disparity optimization stage, the disparity map is optimized with a common local technique, Winner-Take-All (WTA). Then, for final stage, the process continues with post processing that is Left Right (LR) consistency checking. Weighted Median (WM) filter is that applied to secure the final disparity map for noise reduction and smoothening to the disparity map. Based on Middlebury Standard Benchmarking Dataset, the proposed algorithm has 23.35% accuracy for nonocc error and 31.65% accuracy for all error, which yields a better accuracy compared to some works in the evaluation dataset.

[1]*corresponding author*

2020 *Mathematics Subject Classification.* 68U10, 68W99.

Key words and phrases. computer vision, image processing, stereo matching algorithm.

Submitted: 07.01.2021; *Accepted:* 22.01.2021; *Published:* 09.02.2021.

1. INTRODUCTION

One of the key topics in computer vision is a stereo vision that signifies a system to measure depth estimation from 3D information extraction from digital stereo images pair. The framework to obtain the disparity map is called a stereo matching algorithm, widely studied by researchers concentrating to the improve disparity accuracy [1]. Disparity map represents the depth measurement of map that can be used for several applications, such as 3D image reconstruction, medical image processing, 3D entertainment and many more [2]. Traditional taxonomy to produce disparity map consists of matching cost computation, cost aggregation, final disparity selection and disparity refinement. In a stereo vision, the optimization of each disparity map taxonomy mainly grouped into three methods; local, global and semiglobal [3]. These methods can be classified based on the way how the disparity is estimated. The local method provides a simple cost computational due the method uses comparing pixel process that from only information of nearby pixel each other thus make it involves shorter processing time. Whereas global method mostly delivers high disparity map accuracy by identifying all the disparities in the system through energy function minimization at the same time. However, the trade-off of this method are making it requires longer processing, complex and cost expensive. Another of method is the semiglobal that is the integration of both local and global approach, mostly produce balance result and varies depending on the composition and approach applied.

In this work, a new composition of local method of stereo vision algorithm is proposed to enhance the disparity accuracy of local method. The algorithm used the image pairs form Middlebury Stereo Vision database, a standard benchmarking dataset as the stereo images input [4]. Furthermore, fifteen sets of stereo images were processed, which are then work on the proposed stereo algorithm for final disparity maps. While the traditional stereo vision taxonomy started with the matching process, this algorithm proposed a pre-processing stage to enhance the stereo images before the matching process. The pre-processing stage used two different approaches; CLAHE and the AGCWD with combination of guided filter to smooth the surface the same time enhance the low texture and edge regions. The matching cost computational process apply the Census Transform (CT). The CT reduces the effects from radiometric changes in RGB

colour space, and they are used to generate feature points and to calculate the cost of the corresponding matching points between reference and target images. Candidate matching selects the candidate points, and propagation uses the result of the candidate matching to produce a rough disparity map. The cost aggregation stage uses combination of fixed window and guided filter. Then, a Winner-Take-All (WTA) approach is utilized for disparity selection which require less processing time, complexity and cheaper. Finally, the post processing technique in disparity refinement stage consists of left-right consistency check and Weighted Median Filter (WMF) are applied to remove, reduce and smoothening the noises in disparity map. The accuracy result of the stereo vision algorithm is assessed by submitting to the online Middlebury standard benchmarking dataset for qualitative and quantitative result. The evaluation of the result is based on the image quality parameters, overall bad pixel error and non-occluded error.

2. Enhancement Architecture

The information of colour image is richer compare with the gray images. In recent years a lot of researcher applying the colour images in several studies for application such as visual surveillance, electronic consumer and traffic analysis. However, in real practical application, colour images obtained are consists with noises due to undesirable weather and illumination conditions [5]. These images that taken under inadequate or non-uniform light contribute to low brightness, blurred local details, poor contrast and colour fidelity and noise from sudden changes in light make it problematical to analyse and obtain the information.

2.1. **Contrast Limited Adaptive Histogram Equalization.**

Despite the jargon, the framework of CLAHE is straightforward, starting with image decomposition into rectangular blocks [6]. The second step is adjusting to each histogram block, including creating, clipping, and distributing the histogram. The third step is to obtain the cumulative distribution function (CDF) and the probability density function (PDF) of the clipped histogram. Finally, the equalization mapping done by the bi-linear interpolation is executed amongst the blocks to eliminate potential block artefacts and avoid visibility of region boundaries. The bins are established at 180 after a series of segmentation and histogram shape

distribution specified as Rayleigh to create a bell-shaped histogram. This technique improves conventional HE by controlling the contrast utilizing a clip point to chop off the histogram peak value in each block. Therefore, the clip point is an essential factor in terms of the contrast factor that avoids the image's oversaturation precisely inhomogeneous areas. The clipped pixels are redistributed to each gray level. The clip point Equation (2.1) is calculated as follows [7]:

$$B = (\frac{M}{N}(1 + \frac{\alpha(S_{max})}{100})), \tag{2.1}$$

where M represents each block number of pixels while N represents the dynamic block range. α is the clip factor, and S is the maximum slope. The critical factor is the clip point in the contrast enhancement adjustment. The clip limit for this experiment is adjusted to a value of 0.009. The equation of mapping function used to remap the image blocks gray levels is based on the CDF and PDF provided from the clipped histogram as in Equation (2.2) and (2.3),

$$CDF(I) = \sum_{k=0}^{I} PDF(I) \tag{2.2}$$

$$T_{map}(I) = CDF(I) \times I_{max}, \tag{2.3}$$

where Tmap(I) is the remapping function while I is the gray level pixel, and Imax is the block maximum pixel value. In general, this is attractive because it is very fast to compute for different mapping functions based on the CDF of histogram redistribution for each block. The remapped of pixel p using the bilinear interpolation in the equalization mapping step as follows Equation (2.4):

$$\begin{aligned} T_{map}(p(i)) = m.(n.T_a, p(i) + (1-n).T_b.p(i)) + (1-m).(n.T_c.p(i)) \\ + (1-n).T_d.p(i). \end{aligned} \tag{2.4}$$

The p is the arbitrary pixel surrounding the four blocks while points a, b, c, and d are the four blocks' center pixels. T (·) denotes the remapping function, whereas p(i) is the value of an arbitrary pixel i with coordinate (x, y). This interpolation step is essential for making the method feasible for a low computational cost for image enhancement, and the stage also removes blocking artefacts.

2.2. **Adaptive Gamma Correction Weighted Distribution.** The AGCWD technique has been used extensively to solve the problem of manually gamma value adjustment for image enhancement [8]. The weighted distribution function in AGCWD will improve the algorithm to obtain the values automatically. The straightforward formula of the transform-based of gamma correction is derived by Equation (2.5). The proposed AGCWD algorithm is expressed as follows:

$$T_c(I) = I_{max}(\frac{I}{I_{max}})^{1-CDF(I)} \tag{2.5}$$

and

$$PDF_c(I) = PDF_{max}(\frac{PDF(I) - PDF_{min}}{PDF_{max} - PDF_{min}})^{\alpha},$$

where PDFmax and PDFmin are the maximum and minimum PDF of the statistical histogram from histogram analysis, whereas α is the weighted adjusted parameter. In this experiment, the α is manual adjusted to 0.5. This approach requires that an optimal solution be reached using the Recursively Separated and Weighted Histogram Equalization (RSWHE) method. The next step is to calculate the approximation CDF as follows in Equation (2.6):

$$CDF_w(I) = \frac{\sum_{l=0}^{I} maxPDF_w(I)}{\sum PDF_w}. \tag{2.6}$$

2.3. **Guided Filter.** In this experiment, a guided filter setup was implemented to aid in developing and testing these techniques to smooth the image enhancement. As well as being simple, the method is practical and thus is suitable for better preserves the sharpness of image edges. The guided image filtering is applied to each channel independently of the colour images. The guided image filter local linear model in Equation (2.7) of the multi channels as follows [9]:

$$a_k = (\sum_k + \epsilon \cup)^{-1}(\frac{1}{\omega}\sum_{i \in \omega_k} I_i p_i - \mu_k \overline{p_k}) \tag{2.7}$$

is the 3 x 3 matrix identity and $\sum_k$ is the 3 x 3 matrix co-variance. It appears that this filter generally produces better results to preserve edges that are not apparent on grayscale. Thus, the experiment value of the degree of smoothing on the filter is 650.25, which indicates a soft threshold on variance for the given neighbourhood.

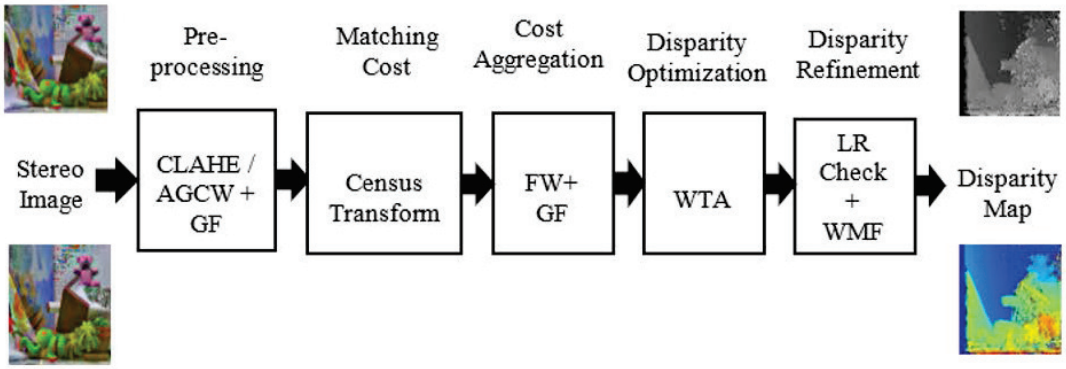

FIGURE 1. Block diagram for proposed algorithm.

3. METHODOLOGY

The proposed stereo vision algorithm has been processed through five stages and the block diagram of the algorithm is presented in Figure 1. The algorithm begins with pre-processing stage to enhance the colour image quality using combination of CLAHE, AGCWD and guided filter. Then, the matching cost computation are done using the Census Transform approach. Census Transform has a strong advantage in radial distortion and brightness changes. The third stage will produce the aggregated cost from matching process utilizing fixed-window and guided filter technique. At the fourth stage; disparity optimization stage, the disparity map is optimized with a common local technique, Winner-Take-All (WTA). Then, for final stage, the process continues with post processing that is Left Right (LR) consistency checking. Weighted Median (WM) filter is that applied to secure the final disparity map.

3.1. **Pre-processing.** This stage provides the method to implement the colour image enhancement algorithm based on CLAHE and AGCWD with guided filtering as shown in Figure 2. The dataset stereo pair images are from The Middlebury Stereo Vision Page that provides 15 stereo pair images in training sets with different resolutions, disparity level, height, width, image size, and camera calibration parameters [10]. A comprehensive explanation of each stage for the developed techniques is given in the following sub-sections. The Block diagram of the developed methods is shown in Figure 2. The experiments have been conducted to be comparable for the visual quality with quantitative analysis within

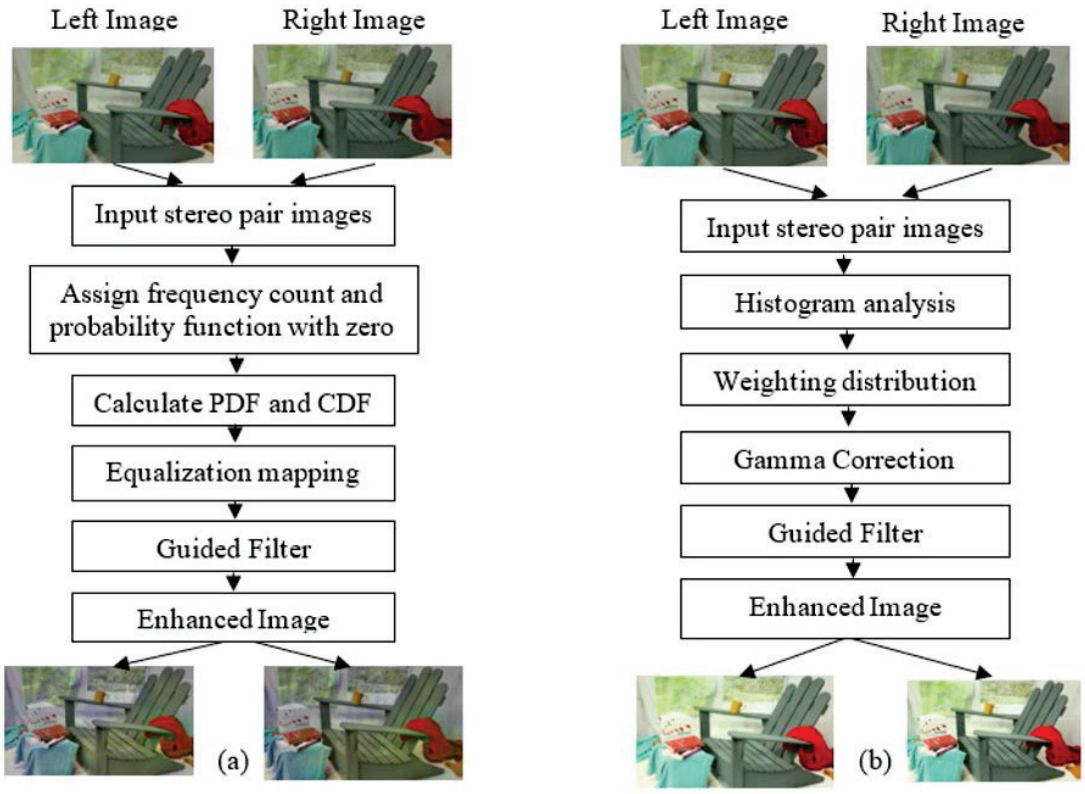

FIGURE 2. Proposed pre-processing method (a) CLAHE and guided filtering (b) AGCWD and guided filtering

five categories; 1. Original image, 2. CLAHE, 3. AGCWD, 4. CLAHE + GF, and 5. AGCWD + GF.

3.2. **Matching cost computation.** Census Transform is a non-parametric local transform that based have characteristic of local intensity relationship between center pixel with neighbour pixels within a census window [11]. The census window can be presented as $(2m+1) \times (2n+1)$ so the transform can be defined as Equation (3.1):

$$T(x,y) = \otimes_{i=-n}^{n} \otimes_{i=-m}^{m} \xi(I(x,y), I(x+i, y+i)), \tag{3.1}$$

where the intensity for pixel (x,y) represents by I(x,y) and the operator of $\otimes$ denotes a bit wise catenation.

3.3. **Cost Aggregation.** The correspondence of a pixel can be determined from CT matching cost by computing the window costs for all candidate in the reference image to the target image. The target image provide the best window cost to corresponding of the reference image. In the cost aggregation step, a square-fixed-window implemented using box filter technique [4]. The window size is set to $(2r+1) \times (2r+1)$ so that the aggregated cost can be determined using Equation (3.2) and (3.3):

$$T^r(u,v,d) = \frac{1}{2r+1} \sum_{m=-r}^{r} C(u+m,v,d) \tag{3.2}$$

$$A^r_{square}(u,v,d) = \frac{1}{2r+1} \sum_{n=-r}^{r} C(u,v+n,d), \tag{3.3}$$

where Tr is the cost matrix holding the intermediate results. It is assuming that the stereo images are rectified, which means that the corresponding epipolar lines are horizontal and on the same height. Then, the aggregated cost value will be smoothed with guided filter.

3.4. **Disparity selection.** To obtain the local approach's accurate disparity map, this work computes the final disparity by selecting a minimum aggregated corresponding value for each pixel using the WTA strategy. The utilization of the WTA strategy for local algorithms can reduce the computational complexity as implemented by [12] and [13]. However, through their findings, the disparity maps attained at this stage still having errors in the occluded or low texture areas. The WTA equation is given by Equation (3.4).

$$d = argmin_{d \in d_r} A^r_{square}(u,v,d), \tag{3.4}$$

where the disparity associated with the minimum aggregated cost d at each pixel is chosen. The $A^r_{square}(u,v,d)$ means the cost aggregation volume from Equation (3.3) and represents the range of allowed disparity values in an image.

3.5. **Disparity refinement.** The final stage of the proposed algorithm consists of post-processing steps. It comprises several consecutive processes: occlusion handling and invalid disparity detection, invalid fill-in disparity, and filtering process. The occlusion and invalid disparity locations are detected by the Left-Right consistency checking process. This process is performed from the left reference disparity map image that coincides with the right reference disparity

map. The output is the invalid disparity locations, which do not have the consistent value of disparities between the two maps. Therefore, using the same approach used by [14] and [15], the location for disparity validation map do at point p is determined by Equation (3.5):

$$d_0(u,v) = \begin{cases} 1, & \text{if } |d_{LR}(u,v) - d_{RL}(u,v)| \leq \tau_{LR} \\ 0, & \text{otherwise} \end{cases}, \tag{3.5}$$

where dLR denotes the left reference and dRL is the right reference of disparity maps. This map contains the invalid (i.e., 1=outlier) and valid (i.e., 0=inlier) disparity locations. Following the same setting with [15], in this work the τLR is set to zero. This is to get the minimum error in the disparity map. To remove the noise, the weighted median filter using B(p;q) is utilized. The weighted median filter was implemented in [16]. Their approaches achieved high accuracy on noise removal. According to this, from Equation (3.5), the weighted of B(p, q) is changed to a summation of histogram h(u,v, dr), which produces Equation (3.6):

$$h(u,v,d_r) = \sum_{q \in w_p | d(q) = d_r} B(u,v,q), \tag{3.6}$$

where dr denotes the disparity range (i.e., dr $\in$[disparity range]), and wp is the window size with the radius r x r at centered pixel of p or at the coordinates (u,v). The final disparity value d' is determined by the median value of $h(u,v,dr)$ given by Equation (3.7):

$$d' = \text{med}\, d | h(p,d_r). \tag{3.7}$$

3.6. **Performance parameter and evaluation.** Each technique's performance is compared to qualitatively and quantitatively through image quality parameters of Entropy, MSE, PSNR and histogram calculation, and visual inspection evaluation [17]. Entropy is also referred to as the overall amount of information details in the image and expressed in bits, and describes the amount of uncertainty gray levels measurement in the input image. The formulated of the Entropy based on Shannon is given below Equation (3.8):

$$E(p) = \sum P(k) \times \log P(k), L = 1, k = 0, \tag{3.8}$$

where P(k) is the probability of gray levels with intensity l and L is the total number of gray levels present in the image. Additional, two typically employed

measurements are PSNR and MSE. The MSE and PSNR between the two images are as follows Equation (3.9) and (3.10):

$$MSE = \frac{1}{MN} \sum_{N=1}^{M} \sum_{M=1}^{N} [\overline{g}(n,m) - g(n,m]^2, \tag{3.9}$$

$$PSNR = 10 \log_{10} \frac{MSE}{s^2}, \tag{3.10}$$

where S is the maximum value of pixel. The higher the PSNR, the better the quality of the image contrast enhancement. Both of these parameters are used to compare image enhancement quality. It is vital to measure the performance's variability apart from that qualitative evaluation to review developed image enhancement performance [18]. The visual quality evaluation technique has been included. For quantitative evaluation and qualitative analysis of the stereo algorithm performance, the Middlebury Vision Benchmark Dataset for stereo matching will be utilized for measuring the bad pixel error percentage. Middlebury dataset was developed by [10] which consists of 15 training images.

4. Results and discussion

The anticipated result of this research effort are to produce a new composition of stereo matching algorithm consists of a new pre-processing step with the overall stereo matching algorithm. It is competent to enhance the edge-preserving properties in the disparity map produced and strong against the repetitive and low texture regions. The final output of this algorithm is the disparity map and the performance is compared to other stereo matching approach around the world through standard online benchmarking system.

4.1. **Pre-processing quality evaluation.** Several quantitative parameters are used to analyse data for image contrast enhancement performance by calculating the Entropy, MSE, PSNR, and histogram distribution. Most data used in the study have been obtained from algorithm execution, and the comparative analysis of average value in each category have been presented in Table 1. Experimental results reveal the AGCWD offers performance advantages on providing the maximum Entropy which is almost equal to Entropy of original input

images and greater than that of Entropy of other techniques; CLAHE as tabulated at 101.3% for AGCWD and 101.1% for AGCWD + GF whereas CLAHE only contributed 100.2% and CLAHE + GF at 99.9% still good for the enhancement. However, entropy evaluation for several individual images under AGCWD and

TABLE 1. Average Entropy, MSE and PSNR.

Parameter	Entropy					MSE				PSNR			
Image Type	Original	CLAHE	AGCWD	CLAHE + GF	AGCWD + GF	CLAHE	AGCWD	CLAHE + GF	AGCWD + GF	CLAHE	AGCWD	CLAHE + GF	AGCWD + GF
Adirondack	7.3597	7.2671	7.7043	7.2396	7.7322	258.55	1976.10	258.27	1969.15	24.02	15.18	24.03	15.20
ArtL	7.6888	7.6608	7.8910	7.6336	7.9123	364.91	1506.25	367.24	1488.70	22.52	16.38	22.50	16.43
Jadeplant	7.4567	7.5175	7.5366	7.4836	7.5432	591.39	590.02	589.62	592.13	20.41	20.42	20.43	20.41
Motorcycle	7.8242	7.7562	7.9222	7.7428	7.9424	410.82	1300.45	420.83	1290.20	22.00	16.99	21.89	17.02
MotorcycleE	7.6946	7.6645	7.8738	7.6497	7.9048	615.28	1655.35	621.84	1637.20	20.47	16.04	20.41	16.09
Piano	7.5461	7.5399	7.6912	7.5478	7.7228	613.35	910.41	612.75	909.02	20.25	18.54	20.26	18.55
PianoL	7.5265	7.5384	7.7638	7.5284	7.7968	568.52	1387.37	567.80	1381.18	20.60	16.96	20.61	16.98
Pipes	7.4255	7.5957	7.7761	7.5720	7.8185	533.78	1645.85	537.38	1614.25	20.87	15.97	20.84	16.05
Playroom	7.7527	7.7835	7.7939	7.7652	7.8127	559.85	977.04	568.57	972.17	20.65	18.25	20.58	18.27
Playtable	7.7822	7.7893	7.7662	7.7451	7.7672	388.16	935.61	391.93	923.14	22.24	18.42	22.20	18.48
PlaytableP	7.7775	7.7856	7.7673	7.7399	7.7685	386.56	942.50	390.34	929.52	22.26	18.39	22.22	18.45
Recycle	7.5499	7.4249	7.5386	7.4115	7.5525	681.31	1071.70	681.61	1071.05	19.80	17.83	19.80	17.83
Shelves	7.5270	7.4300	7.7682	7.4027	7.7909	179.33	1722.95	183.90	1717.05	25.61	15.77	25.50	15.78
Teddy	7.7903	7.7253	7.8693	7.6924	7.8769	419.14	1154.10	423.99	1162.30	21.91	17.51	21.86	17.48
Vintage	7.0895	7.5150	6.5670	7.4843	6.0802	958.56	460.38	960.41	477.94	18.32	21.50	18.31	21.34
Avg	**7.5861**	**7.5996**	**7.6819**	**7.5759**	**7.6681**	**501.97**	**1215.74**	**505.10**	**1209.00**	**21.46**	**17.61**	**21.43**	**17.62**

AGCWD + GF, especially for low texture images, show a slightly lower entropy result at 85.8% compared with the original images. One of the most critical findings relates to the MSE and PSNR results for CLAHE. CLAHE techniques provide a significant performance increase in comparison to AGCWD in PSNR at 21.9% for CLAHE with AGCWD and at 21.6% for CLAHE + GF with AGCWD + GF linking to lower MSE at 41.3% for CLAHE to AGCWD and at 41.8% for CLAHE + GF to AGCWD + GF. This is an exciting finding, and it could be hypothesized that the CLAHE technique has better enhancement compare with the AGCWD based on the original images.

4.2. **Stereo matching performance.** The experiments are carried out on the platform of Window 10 on desktop PC with 3.2GHz processor and 8GB memory. To evaluate the accuracy, the experimental images are using a standard online benchmarking dataset from the Middlebury. The accuracy is measured from the

bad pixel percentage of non-occluded pixel (nonocc) and all pixels (all). Figure 3 shows the 15 training images, ground truth and the disparity map results after submitted to Middlebury online platform.

Based on the final results of disparity maps, the scene objects situated at increasing depth are assigned step by step to disparity values from nearer to further based on the colours assignment. Table 2 show the quantitative results of the Middlebury dataset. It shows that the proposed work is more accurate than the Census Transform (i.e., with the weight average difference nonocc=3.1, all=2.9). The achievement of the proposed work has been analysed with other local algorithms in Middlebury Dataset. Based on the results, the proposed algorithm is among the lowest of average errors which indicates the competitive achievement of the proposed work.

TABLE 2. The comparison results of nonocc error and all error using Middlebury dataset.

Image Type	CT		SED		MTS		**CLAHE + CT**		**AGCWD + CT**	
	nonocc	all	nonocc	all	nonocc	all	nonocc	all	nonocc	all
Adiron	26.3	30	23.7	25.1	**17.2**	**19**	19.1	23.4	19.1	23.4
ArtL	**6.16**	24.3	15.6	**17.1**	17.3	22.5	9.78	27.4	10.8	27.7
Jadepl	51.1	72.4	106	123	107	123	**42.6**	**64.5**	48.3	69.6
Motor	12.2	19.6	18.3	20.6	14.8	17.5	**9.09**	**16.8**	10.5	18.1
MotorE	11.8	19.2	17.7	19.7	18.3	20.7	**9.27**	**17**	10.7	18.3
Piano	18.7	23.2	17.7	**18.1**	**12.4**	13	16.8	21.3	18.1	22.5
PianoL	**29**	32.7	29.7	**29.5**	32	32	30	33.4	31	34.4
Pipes	17	30	28.5	34.1	22.4	29.4	**12.5**	**26.3**	14.9	28.3
Playrm	28.9	43.5	**21.3**	**22.8**	21.9	26.9	24.2	39.5	24.3	39.6
Playt	37.4	42.6	**18.2**	**18.8**	25.9	27.4	31.6	37.3	33.2	38.7
PlaytP	16.2	22.6	15.9	16.5	**10.3**	**12**	13.7	20.3	15.1	21.5
Recyc	20.5	23.8	16.2	**16.8**	16.4	17.5	**15.3**	19.2	18.9	22.4
Shelvs	28.2	29.9	14.4	**15.1**	**11.47**	12.1	25.3	27.2	25.6	27.4
Teddy	8.96	17.6	**6.65**	**7.26**	6.96	8.11	7.68	16.5	9.89	18.6
Vintge	72.2	75.5	31.6	33.8	**25.2**	**27.2**	70.3	73.8	72.2	75.4
Weight Ave	25.6	33.8	25.4	27.9	24.0	**27.2**	**22.5**	30.9	24.2	32.4

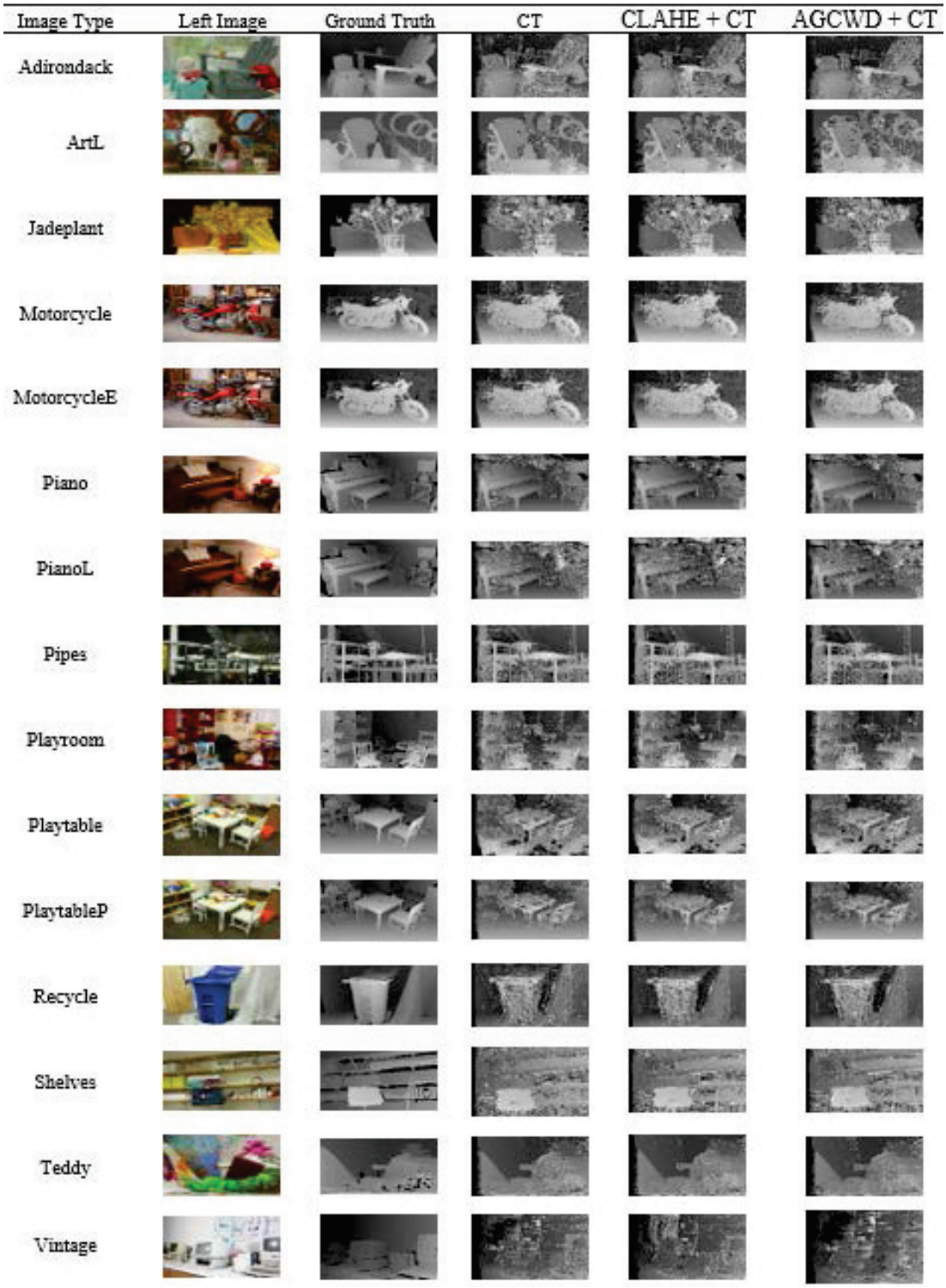

FIGURE 3. Disparity map evaluation using Middlebury training dataset.

In the preliminary experiments, the aim is the integrating the Contrast Limited Adaptive Histogram Equalization (CLAHE), including Adaptive Gamma Correction Weight Distribution (AGCWD) with Guided Filter (GF) for contrast enhancement for stereo pair images in the processing stage. These methods are expected to preserve the maximum entropy and the over enhancement control, and quantitative analysis is performed to measure the enhancement performance. These techniques have demonstrated a marked improvement in stereo vision images' quality more efficiently than the original images. Based on the Entropy, MSE, PSNR, and histogram evaluation, better results and better visual enhancement of the images can be applied to the stereo matching algorithm matching cost computation. After the pre-processing stage, the enhanced image is used in the stereo matching algorithm framework. The algorithm can reduce the errors and increase the accuracy based on the Middlebury dataset. The combination of pre-processing and matching costs in the framework is robust against the radiometric difference, identifying the regions with different brightness. Additionally, the GF can increase the efficiency and preserve the edges of an object. The results of disparity maps have demonstrated that the framework increases the accuracy compared with other stereo matching algorithms.

5. Conclusion

This paper presents several techniques used in the pre-processing step for stereo vision algorithm. The proposed CLAHE and AGCWD techniques are implemented with the combination of a guided filter for image smoothing. The CLAHE technique consisted of assigning the frequency and probability function, calculation of PDF and CDF, and equalization mapping. In contrast, the AGCWD consists of histogram analysis, weight distribution, and gamma correction. These techniques have demonstrated a marked improvement in stereo vision images algorithm accuracy and quality efficiently compared with the several stereo vision methods. Based on the quantitative and qualitative evaluation, better results and better visual enhancement of the images were applied to the stereo vision algorithm. Future developments are intended to improve this algorithm even more with the idea of a hybrid technique for the pre-processing step and the implementation of histogram aggregation strategy.

ACKNOWLEDGMENT

This work was supported by the Universiti Teknikal Malaysia Melaka (UTeM) with a grant number (PJP/2020/FTKEE/TD/S01726).

REFERENCES

[1] R. A. HAMZAH, H. IBRAHIM: *Literature survey on stereo vision disparity map algorithms*, J. Sensors, **2016** (2016), l–22.

[2] P. TAN, P. MONASSE: *Stereo Disparity through Cost Aggregation with Guided Filter*, Image Process. Line, **23**(4) (2014), 252–275.

[3] E. BEBESELEA-STERP, R. R. BRAD, R. R. BRAD: *A Comparative Study of Stereovision Algorithms*, Int. J. Adv. Comput. Sci. Appl., **8**(11) (2017), 359—375.

[4] D. SCHARSTEIN, R. SZELISKI: *A taxonomy and evaluation of dense two-frame stereo correspondence algorithms*, Int. J. Comput. Vis., **47**(1–3) (2002), 7–42.

[5] H. W. JO, B. MOON: *(2016) A modified census transform using the representative intensity values*, ISOCC 2015 - Int. SoC Des. Conf. SoC Internet Everything, pp. 309—310.

[6] M. VELUCHAMY, B. SUBRAMANI: *Image contrast and color enhancement using adaptive gamma correction and histogram equalization*, Optik (Stuttg)., **183** (2019), 329—337.

[7] Y. CHANG, C. JUNG, J. HWANG: *Automatic Contrast-Limited Adaptive Histogram Equalization with Dual Gamma Correction*, IEEE Access, **6** (2018), 11782—11792.

[8] S. C. HUANG, F. C. CHENG, Y. S. CHIU: *Efficient contrast enhancement using adaptive gamma correction*, IEEE Trans. Image Process., **22**(3) (2013), 1032–1041.

[9] Q. MU, Y. WEI, Z. LI: *Color Image Enhancement Method Based on Weighted Image Guided Filtering*, **1** (2018), 1–15.

[10] D. SCHARSTEIN: *High-resolution stereo datasets with subpixel-accurate ground truth*, in German conference on pattern recognition, (2014), 31–42.

[11] J. LIM, S. LEE: *A census transform-based robust stereo matching under radiometric changes*, in Signal and Information Processing Association Conference, (2016), 34–43.

[12] C. CIGLA, A. A. ALATAN: *Information permeability for stereo matching*, Signal Process. Image Commun., **28**(9) (2013), 1072–1088.

[13] T. A. CHANG: *Robust stereo matching with trinary cross color census and triple image-based refinements*, EURASIP J. Adv. Signal Process., **2017(1)**(27) (2017), 87–99.

[14] S. MATTOCCIA, L. DI STEFANO: *(2007) Stereo vision enabling precise border localization within a scanline optimization framework*, in Asian Conference on Computer Vision (2007), 517–527.

[15] G. A. KORDELAS, D.S. ALEXIADIS, E. IZQUIERDO: *Enhanced disparity estimation in stereo images*, Image Vis. Comput., **35** (2015), 31–49.

[16] W. WU, L. LI, W. JIN: *Disparity refinement based on segment-tree and fast weighted median filter*, in International Conference on Image Processing, ICI, (2016), 56–68.

[17] R. KAUR, M. CHAWLA, M. D. ANSARI: *Comparative analysis of contrast enhancement techniques for medical images*, Pertanika J. Sci. Technol., **26**(3) (2018), 965–978.

[18] J. R. TANG, N. A. MAT ISA: *Bi-histogram equalization using modified histogram bins*, Appl. Soft Comput. J., **55** (2017), 31–43.

FACULTY OF ELECTRICAL AND ELECTRONIC ENGINEERING TECHNOLOGY
UNIVERSITI TEKNIKAL MALAYSIA MELAKA, MELAKA, MALAYSIA
Email address: fauzan@utem.edu.my

FACULTY OF ELECTRICAL AND ELECTRONIC ENGINEERING TECHNOLOGY
UNIVERSITI TEKNIKAL MALAYSIA MELAKA, MELAKA, MALAYSIA
Email address: rostamaffendi@utem.edu.my

FACULTY OF ELECTRONIC AND COMPUTER ENGINEERING
UNIVERSITI TEKNIKAL MALAYSIA MELAKA, MELAKA, MALAYSIA
Email address: nurulfajar@utem.edu.my@utem.edu.my

FACULTY OF ELECTRICAL AND ELECTRONIC ENGINEERING TECHNOLOGY
UNIVERSITI TEKNIKAL MALAYSIA MELAKA, MELAKA, MALAYSIA
Email address: mohdsaad@utem.edu.my@utem.edu.my